

Structurally Unique Inhibitors of Human Mitogen-Activated Protein Kinase Phosphatase-1 Identified in a Pyrrole Carboxamide Library

John S. Lazo, John J. Skoko, Stefan Werner, Branko Mitasev, Ahmet Bakan, Fumito Koizumi, Archibong Yellow-Duke, Ivet Bahar, and Kay M. Brummond

The Pittsburgh Molecular Libraries Screening Center (J.S.L., J.J.S., I.B., K.M.B.), University of Pittsburgh Drug Discovery Institute (J.S.L., J.J.S., F.K., A.Y.-D.), I.B., K.M.B.), Departments of Pharmacology (J.S.L., J.J.S., F.K., A.Y.-D.), Chemistry (S.W., B.M., K.M.B.), and Computational Biology (A.B., I.B.), and Center for Chemical Methodologies and Library Development (S.W., K.M.B.), University of Pittsburgh, Pittsburgh, Pennsylvania

Received March 3, 2007; accepted May 29, 2007

ABSTRACT

Mitogen-activated protein kinase phosphatase 1 (MKP-1) is a tyrosine phosphatase superfamily member that dephosphorylates and inactivates cardinal mitogen-activated protein kinase (MAPK) substrates, such as p38, c-Jun NH₂-terminal kinase, and extracellular signal-regulated kinase. Although these MAPK substrates regulate many essential cellular processes associated with human diseases, few pharmacological inhibitors have been described. The lack of readily available selective MKP-1 inhibitors has severely limited interrogation of its biological role and was one rationale for using a recently described tricyclic pyrrole-2-carboxamide library in our screening efforts. In this report we demonstrate the pharmacological richness of the pyrrole carboxamide library by the finding that 10 of 172 members inhibited human MKP-1. Two of the pyrrole carboxamides, PSI2106 and MDF2085, were especially notable in

vitro inhibitors of recombinant human MKP-1 enzyme activity with IC₅₀ values of 8.0 ± 0.9 and 8.3 ± 0.8 μM, respectively. Both showed some selectivity for MKP-1 over the closely related phosphatases MKP-3, Cdc25B, VHR, and PTP1B. Computational examination of the surface properties near the catalytic site revealed that the phosphatases studied differ significantly in their electrostatic potential at the substrate binding site. The compounds inhibited MKP-1 reversibly but displayed mixed kinetics. Phosphatase inhibition was retained in the presence of physiologically relevant concentrations of glutathione. Molecular docking studies suggested that PSI2106 may interact with His²²⁹ and Phe²⁹⁹ on MKP-1. These results reveal the power of using a small focused library for identifying pharmacological probes.

Many contemporary drug discovery efforts exploit either diversity-oriented chemical libraries, which are usually designed to have maximum differences in the core structure, or focused chemical libraries, which are fundamentally designed to emulate the structural properties of previously defined “drug-like” core skeletons with variable appended moieties (Stockwell, 2004). Both approaches are complementary. The University of Pittsburgh’s Center for Chemical Methodologies and Library Development has generated novel chemical libraries containing elements that occupy poorly populated chemical space. One subset that was re-

cently described was based on a tricyclic pyrrole-2-carboxamide scaffold (Werner et al., 2006). This library was of particular pharmacological interest because the pyrrole carboxamide skeleton is unique, has not been well explored, and is a core unit in many marine natural products with experimental antitumor (agelastatin A and yatakemycin), antihistamine (dispacamide A), antiviral (scepterin), or antibacterial (storniamide A) activity (Okano et al., 2006; Werner et al., 2006). In the current study we provide the first documentation of the biological activity of members in this novel pyrrole carboxamide library, which was synthesized using a sequence of three reactions: Pauson-Khand cycloaddition and Stetter and Paal-Knorr condensations (Brummond et al., 2005; Werner et al., 2006).

It is now widely recognized that mammalian cells use mitogen-activated protein kinases (MAPKs) as distal effec-

This work was supported by National Institutes of Health Grants MH074411, GM067982, and CA052995 and by the Fiske Drug Discovery Fund. Article, publication date, and citation information can be found at <http://jpet.aspetjournals.org>. doi:10.1124/jpet.107.122242.

ABBREVIATIONS: MAPK, mitogen-activated protein kinase; MKP-1, mitogen-activated protein kinase phosphatase-1; DSP, dual specificity phosphatase; Erk, extracellular signaling-related protein kinase; OMFP, 3-O-methylfluorescein phosphate; GSH, glutathione; NU-126, 2-((E)-2-(5-cyanobenzofuran-2-yl)vinyl)-1H-indole-6-carbonitrile.

tors for many extracellular growth factors, stress detectors, and drug sensors. MAPKs are activated by intracellular tyrosine kinases and inactivated by mitogen-activated protein kinase phosphatases (MKPs), which are dual specificity phosphatases (DSPs) capable of dephosphorylating both phosphotyrosine and phosphothreonine on the same protein substrate. The most promiscuous of the 11 human MKPs is MKP-1, which can dephosphorylate p38, c-Jun NH₂-terminal kinase and extracellular signaling-related protein kinase (Erk) 1/2 *in vitro*. Surprisingly, the precise determinants of its substrate specificity remain uncertain (Wu and Bennett, 2005), although it regulates cytokine and mitogen response. The crystal or solution structure for MKP-1 is not available to guide any rational inhibitor design. MKP-1 expression is elevated in prostate, breast, gastric, and renal cancer (Magi-Galluzzi et al., 1997; Liao et al., 2003; Wang et al., 2003) and is correlated with decreased progression-free survival (Denkert et al., 2002). Moreover, a reduction in MKP-1 expression by antisense decreases the tumorigenicity of pancreatic cancer cells (Liao et al., 2003). Induction of MKP-1 leads to resistance to therapeutically useful ionizing radiation (Nyati et al., 2006). Consequently, the availability of potent and selective inhibitors of MKP-1 would be quite desirable both as biological reagents to deconstruct the roles of the MKP family members and as possible lead structures for future cancer-directed therapies. Unfortunately, MKP-1 appears to be a challenging pharmacological target for small molecule inhibitors. The limited number of known small molecule MKP-1 inhibitors are either not potent or not selective (Pathak et al., 2002; Vogt et al., 2005; Lazo et al., 2006; Arnold et al., 2007). Therefore, we were inspired to examine the pyrrole carboxamide library from the Center for Chemical Methodologies and Library Development because its members are bisfunctional and are reminiscent of potent inhibitors of other protein tyrosine phosphatases that are postulated to bind to the active site and an adjacent sub-pocket. Moreover, the library has never been systematically biologically evaluated, and its members contain a core structure found in many marine natural products with pharmacological activity. Interestingly, we found that 10 of the 172 pyrrole carboxamide library members inhibited human MKP-1 and that 2 of these are potent and selective. We used contemporary computational methodologies to speculate on the sites of interactions and to guide future synthetic efforts.

Materials and Methods

Chemical and Reagents. The synthesis of the tricyclic pyrrole-2-carboxamide library has been published previously (Werner et al., 2006). Only 172 of the previously published compounds were available in sufficient quantities to permit biological analysis. Epitope-tagged His₆Cdc25B₂, His₆MKP-1, and His₆MKP-3 were expressed in *Escherichia coli* and purified by Ni-NTA as described previously (Lazo et al., 2001). Recombinant VHR and PTP1B were obtained from Biomol (Plymouth Meeting, PA). A549 cells were obtained from American Type Culture Collection (Manassas, VA), and growth inhibition was determined with Alamar Blue (CellTiter-Blue; Promega, Madison, WI). Unless otherwise indicated, all other reagents were obtained from Sigma-Aldrich (St. Louis, MO).

Enzyme Assays. Enzyme activities in the absence and presence of small molecule inhibitors were measured using the artificial substrate 3-*O*-methylfluorescein phosphate (OMFP) at concentrations equal to the K_m of each enzyme and at the optimal pH for individual

enzyme activity as described previously (Lazo et al., 2001). We first evaluated the 172 compounds in the pyrrole carboxamide library for inhibition of MKP-1 at 10 μ M in a 96-well high-throughput screening format. The standard assay condition contained 40 μ M OMFP in an assay buffer comprising 30 mM Tris-HCl (pH 7.0), 75 mM NaCl, 1 mM EDTA, 0.33% bovine serum albumin and 1 mM dithiothreitol. Fluorescence emission from the product was measured after a 60-min incubation period at ambient temperature with a multiwell plate reader (Cytofluor II, excitation filter, 485 nm/20 nm bandwidth; emission filter, 530 nm/30 nm bandwidth; Applied Biosystems, Foster City, CA). Compounds that inhibited MKP-1 by >50% in the initial screen were reassayed for IC₅₀ values, which were determined from two independent experiments using samples of eight concentrations ranging from 0.78 to 100 μ M. Data were analyzed with Prism 3.0 (GraphPad Software, Inc., San Diego, CA). Unbiased assignments for the best-fit model were determined using Enzyme Kinetics Module 1.0 (SPSS Inc., Chicago, IL). For the reversibility studies, we used a previously described dilution method (Brisson et al., 2005). Briefly, the enzyme and 90 μ M PSI2106, MDF2085, or vehicle control were preincubated for 0, 5, or 20 min and then diluted 20-fold with incubation buffer. The OMFP substrate was added, and the remaining enzyme activity was determined and compared with the vehicle control sample. For the reductant studies, 1 to 25 mM glutathione was added during the incubation period.

Inhibition of Erk dephosphorylation was determined by incubating recombinant His₆-tagged MKP-1 (125 ng) with tyrosine- and threonine-phosphorylated Erk2 (10 ng; New England Biolabs, Ipswich, MA) in a final reaction mixture (15 μ l) containing 30 mM Tris-HCl, pH 7.0, 75 mM NaCl, 0.67 mM EDTA, 1 mM dithiothreitol, and 0.033% bovine serum albumin. PSI2106 or MDF2085 (6.3–50 μ M), sanguinarine (50 μ M), or dimethyl sulfoxide vehicle control was added, and after incubation for 60 min, Erk dephosphorylation was determined by Western blotting using 10% Tris-glycine gels and a monoclonal phospho-p44/42 MAPK antibody (catalog no. 91065; Cell Signaling Technology Inc., Danvers, MA) at 1:1000 dilution.

Molecular Modeling and Docking Studies. The active catalytic domain structures of MKP-1 and MKP-3 were modeled on the basis of that of MKP-5 deposited in the Protein Data Bank (Protein Data Bank code: 1ZZW) (Jeong et al., 2006). Homology modeling was possible, given that the target and template structures had sufficiently high sequence identity: MKP-1 and MKP-5 have 44% amino acid sequence identity (56% identity around the active site) and MKP-3 and MKP-5 have 48% sequence identity (66% identity around the active site). Models were generated using MODELLER 8v2 (Sali and Blundell, 1993) and refined using AMBER force field implemented in SYBYL 7.2 (Tripos, Inc., St. Louis, MO). The small molecule inhibitors examined (Table 1) were docked onto model structures, as well as known Cdc25B and VHR structures, using a two-step protocol. First, by using AutoDock 3.05 (Morris et al., 1998), an unbiased docking was performed in which the whole catalytic domains were targeted to identify potential binding sites. Then, by using GOLD 3.1 (Jones et al., 1997), flexible side-chain docking was performed to characterize optimal binding poses of the inhibitors. The electrostatic potentials of the solvent-exposed surfaces of the four DSPs were calculated using APBS software (Baker et al., 2001).

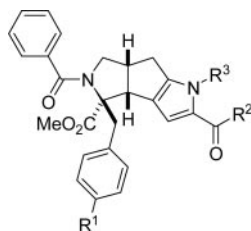
Results

An initial analysis of the pyrrole carboxamide library revealed that 22 of the 172 members inhibited MKP-1 *in vitro* with IC₅₀ values of <30 μ M (Table 2), which was a remarkably high positive rate from a chemical library and documented the benefits of the focused library approach. A further analysis of the 10 compounds with IC₅₀ values for MKP-1 of <10 μ M indicated that several were selective for this phosphatase compared with other related phosphatases,

TABLE 1

Structures of tricyclic pyrrole carboxamide inhibitors of MKP-1

The chemical composition and synthesis of all compounds described in this manuscript has been published elsewhere (Werner et al., 2006), but the nomenclature for individual compounds used herein has been revised for simplicity and convenience as follows: PSI2106, **17** (2,1,27); MDF2085, **17** (2,1,19); MDF2081, **17** (2,1,41); PSI2107, **17** (2,1,21); MDF2061, **17** (3,1,31); MDF2014, **17** (3,2,30); MDF2075, **17** (2,2,19); MDF2050, **17** (3,2,41); STW1192, **17** (2,2,17); and MDF2060, **17** (3,1,34).



Compound	R^1	R^2	R^3
PSI2106	F		
MDF2085	F		
MDF2081	F		
PSI2107	F		
MDF2061	OMe		
MDF2014	OMe		
MDF2075	F		
MDF2050	OMe		
STW1192	F		
MDF2060	OMe		

such as MKP-3, Cdc25B, PTP1B, or VHR (Tables 3 and 4). Of particular note were PSI2106 and MDF2085, which had IC_{50} values of 8.0 ± 0.9 and 8.3 ± 0.8 , respectively. All of the 10

inhibitors possess groups at the *para* position of the aryl ring that are inductively electron withdrawing ($R^1 = \text{OMe}$ or F). Both pyrrolidine and *N,N*-dimethyl substitutions were ac-

TABLE 2

Heat map of inhibitory activity of compounds in the pyrrole carboxamide discovery library

Compounds found in the initial screen to inhibit MKP-1 by >50% were examined with a full concentration-response curve. The bar at the bottom indicates the color code: green, $IC_{50} < 10 \mu M$; yellow, $IC_{50} 10-20 \mu M$; red, $IC_{50} 20-30 \mu M$; gray, no activity (NA); white, no compound (NC).

Compound ^a	8{1}		8{2}		8{3}	
	9{1}	9{2}	9{1}	9{2}	9{1}	9{2}
10{1}						
10{2}						
10{3}						
10{4}						
10{5}						
10{6}						
10{7}						
10{8}						
10{9}						
10{10}						
10{11}						
10{12}						
10{13}						
10{14}						
10{15}						
10{16}						
10{17}						
10{18}						
10{19}						
10{20}						
10{21}						
10{22}						
10{23}						
10{24}						
10{25}						
10{26}						
10{27}						
10{28}						
10{29}						
10{30}						
10{31}						
10{32}						
10{33}						
10{34}						
10{35}						
10{36}						
10{37}						
10{38}						
10{39}						
10{40}						
10{41}						

μM	<10	10-20	20-30	NA	NC
IC_{50}					

^a The nomenclature is according to Werner et al. (2006).

ceptable in the R^2 position, whereas a wide variety of heterocyclic moieties were found on the R^3 position. The pyrrole carboxamide library contained 41 building blocks for the R^3 position; these included aliphatic as well as aromatic and heteroaromatic functionalities and lipophilic as well as hydrophilic ones. Interestingly, all inhibitors contained an aromatic or heteroaromatic ring system in this position, and all

TABLE 3

Potency and selectivity of pyrrole inhibitors of human MKP-1

Ten library compounds from the discovery library exhibited IC_{50} values $< 20 \mu M$. These were examined for selectivity against related human protein tyrosine phosphatases using an identical small molecule substrate, *O*-methyl fluorescein phosphate, as described under *Materials and Methods*. All IC_{50} values were determined using a range of eight concentrations from 0.78 to $100 \mu M$. Mean \pm range; $n = 2$.

Compound	MKP-1	MKP-3	Cdc25B	PTP1B	VHR
PSI2106	8.0 ± 0.9	43.2 ± 0.7	>100	>100	>100
MDF2085	8.3 ± 0.8	58.1 ± 1.6	>100	>100	>100
MDF2081	9.1 ± 2.4	N.D.	N.D.	N.D.	N.D.
PSI2107	10.4 ± 0.9	N.D.	N.D.	N.D.	N.D.
MDF2061	13.9 ± 3.8	42.6 ± 8.4	>100	>100	>100
MDF2014	13.9 ± 1.1	N.D.	N.D.	N.D.	N.D.
MDF2075	16.6 ± 0.9	N.D.	N.D.	N.D.	N.D.
MDF2050	17.0 ± 1.2	79.0 ± 11.6	>100	>100	>100
STW1192	17.6 ± 0.5	37.4 ± 2.7	>100	>100	>100
MDF2060	19.9 ± 0.9	N.D.	N.D.	N.D.	N.D.

N.D., not determined.

of them were substituted in the *ortho* and/or *meta* position. Although a variety of substituents in R^1 and R^2 positions were tolerated, a more specific substitution pattern in the R^3 position was required.

The physicochemical properties of the 172 pyrrole carboxamide library members were evaluated previously (Werner et al., 2006). Using an identical computational analysis, we identified only 1 of the 10 inhibitors, namely MDF2050, that was significantly different from the mean values of the overall population for molecular mass and molecular volume (Table 4). All 10 compounds shared similar computational attributes with previously defined "drug-like" compounds with the exception of the calculated partition coefficient (log P), aqueous solubility (log S) and serum protein binding (log K_{hsa}). All three of these calculated properties were frequently violated in this pyrrole carboxamide library (Werner et al., 2006).

Some protein tyrosine phosphatases appear to be highly sensitive to oxidants, such as H_2O_2 or quinones, because of the low pK_a of the catalytic cysteine (Brisson et al., 2005). To exclude the possibility that inhibition by the pyrrole carboxamides was secondary to simple oxidation, we evaluated the reversibility of enzyme inhibition in the presence or absence of the physiological reductant GSH. Both PSI2106 and MDF2085 retained significant inhibition in the presence of 1 to 25 mM GSH (Fig. 1). This lack of a marked increase in IC_{50} values with increasing amounts of reducing agent suggested that the inhibitors were not acting simply through oxidation-reduction mechanisms.

Because of the initial positive evaluation of PSI2106 and MDF2085, we examined the reversibility and kinetics of inhibition with the small molecule substrate OMFP. Reversibility of inhibition was determined using a dilution method described previously (Brisson et al., 2005). As indicated in Fig. 2A, preoccupation with either pyrrole carboxamide for up to 20 min did not alter the percent inhibition of MKP-1. We next formally determined the kinetics of inhibition and found that both PSI2106 and MDF2085 had calculated K_i values below $10 \mu M$ with mixed kinetics, exhibiting both competitive and noncompetitive properties (Fig. 2, B and C). These results would be consistent with the two compounds interacting at sites near or outside of the catalytic domain and could reflect the bisfunctional nature of the compounds and the possible presence of a second subpocket common to some tyrosine phosphatases. Because some MKPs assume an

TABLE 4

Computational analysis of molecular descriptors for the tricyclic pyrrole carboxamide inhibitors of MKP-1

Parameters were determined as described previously (Werner et al., 2006) using QikProp 2.1 (Schrodinger, Inc., New York, 2003) (Duffy and Jorgensen, 2000; Jorgensen, 2004). FISA is the hydrophobic component of the solvent accessible surface area using a probe with a 1.4-Å radius. Compounds computationally found to be outside of the range for 95% of all drugs based on QikProp 2.1 are indicated in boldface.

Compound	Mol. Wt.	Volume ^a	FISA ^b	No. Rotatable bonds	No. Hydrogen Bond Donors	No. Hydrogen Bond Acceptors	Log P (Octanol/Water)	Log S (Aqueous Solubility)	Log Kh _{SA} (Serum Protein Binding)	Caco Permeability	MDCK ^c Permeability	No. Primary Metabolites
	g/mol	Å ³	Å ²							nm/s		
PSI2106	664.6	1675.3	41.0	7	0	9	6.97	-7.13	1.27	4541	>10,000	4
MDF2085	629.7	1775.9	33.1	7	0	9	8.43	-9.55	2.11	2277	2177	5
MDF2081	725.2	1920.2	50.4	10	1	9	8.41	-8.94	1.86	3541	>10,000	5
PSI2107	682.1	1836.7	26.9	7	0	8	8.42	-9.691	1.77	6612	>10,000	5
MDF2061	671.7	1904.3	27.5	8	0	8	8.69	-10.06	1.94	6512	>10,000	5
MDF2014	667.8	1956.8	36.4	8	0	8.7	8.30	-9.22	1.90	5138	2499	5
MDF2075	655.7	1851.7	33.9	7	0	8	8.16	-9.29	1.82	5488	>10,000	5
MDF2050	763.3	2025.8	53.9	11	1	9.7	8.54	-9.14	1.95	3223	>10,000	6
STW1192	681.7	1872.0	31.8	7	0	10.4	6.97	-7.71	1.24	5801	8946	5
MDF2060	714.7	1958.7	30.6	10	0	9.5	8.01	-9.04	1.62	5987	7242	6

^a Total solvent-accessible volume using a probe with a 14-Å radius (Werner et al., 2006).

^b Hydrophilic component of the solvent-accessible surface area (Werner et al., 2006).

^c MDCK, Madin-Darby canine kidney cells.

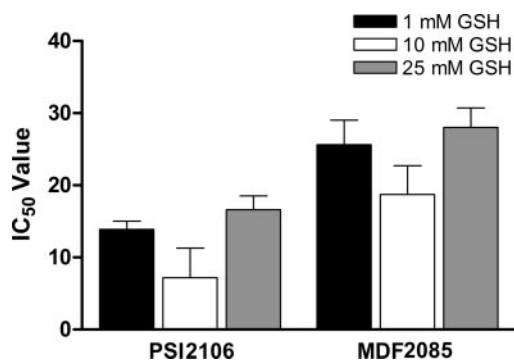


Fig. 1. Effect of GSH on MKP-1 inhibition. MKP-1 was incubated with various concentrations of PSI2106 or MDF2085 and 1, 10, or 25 mM GSH, and the resulting IC₅₀ values were determined using the standard MKP-1 phosphatase assay. Results are means ± S.D.; *n* = 3.

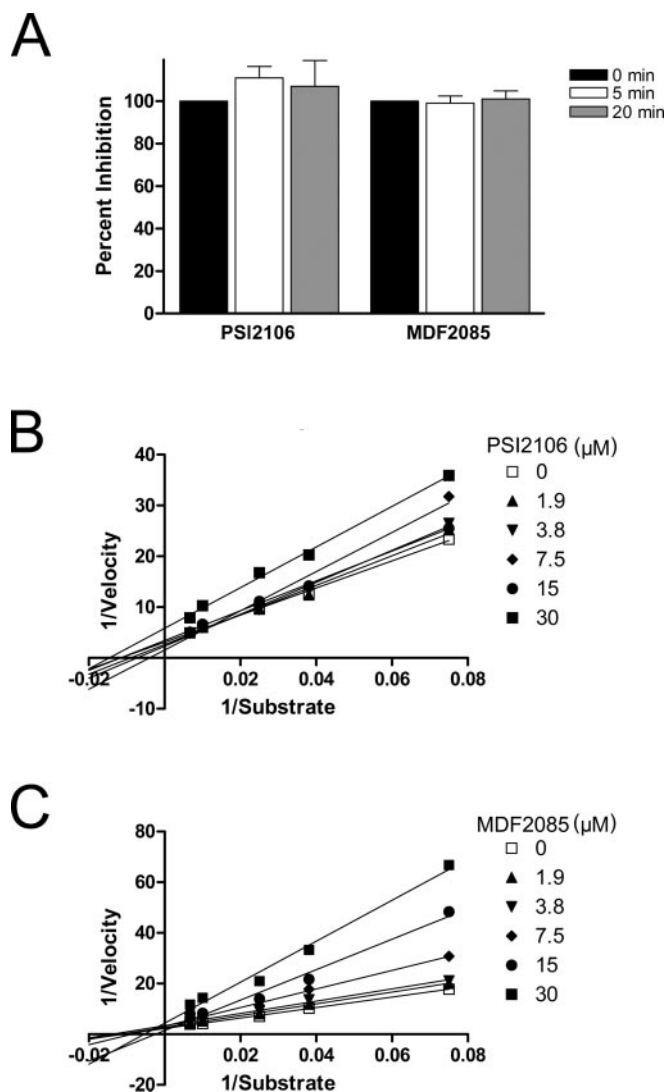


Fig. 2. Reversibility and kinetics of MKP-1 inhibition. A, reversibility studies of PSI2106 and MDF2085 inhibition. MKP-1 was preincubated with 90 μM PSI2106 and MDF2085 for 0 to 20 min and diluted 20-fold with incubation buffer; activity was determined as described previously (Lazo et al., 2006). B, Lineweaver-Burk inhibition plot of PSI2106 with MKP1. Competition was determined using SigmaPlot 2000 with the enzyme kinetics module. A range of five different concentrations of inhibitor from 1.9 to 30 μM were used at five different substrate concentrations. $K_i = 4.3 \pm 0.6 \mu\text{M}$; *n* = 2. C, Lineweaver-Burk inhibition plot of MDF2085 with MKP1. $K_i = 6.0 \pm 1.0 \mu\text{M}$; *n* = 2.

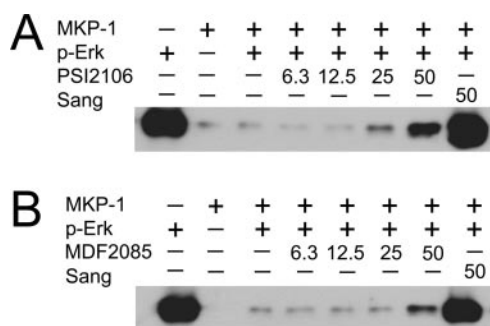


Fig. 3. Inhibition of MKP-1 dephosphorylation of phospho-Erk. Phosphorylated Erk (0.67 $\mu\text{g/ml}$) was incubated with recombinant MKP-1 in the absence or presence of 0 to 50 μM enzyme inhibitors. After incubation, Erk was separated from other proteins by SDS-polyacrylamide gel electrophoresis and transferred to a 0.2- μm nitrocellulose membrane; the phosphorylation status of Erk was determined using an antibody to phosphorylated Erk. A, inhibition with PSI2106. B, inhibition with MDF2085. Concentration units are micromolar concentrations. Sang, sanguinarine, a known nonspecific inhibitor of MKP-1 (Vogt et al., 2005).

altered conformation and are activated after binding to their cognate substrate (Camps et al., 1998; Zhou et al., 2001), we examined the ability of PSI2106 and MDF2085 to inhibit the dephosphorylation of the phosphorylated Erk (Fig. 3). PSI2106 caused a concentration-dependent inhibition of Erk dephosphorylation but was not as effective as sanguinarine, a previously reported inhibitor of MKP-1 (Vogt et al., 2005). MDF2085 also inhibited the dephosphorylation of the protein substrate, but it was less effective than PSI2106.

To assist in understanding the potential specificity PSI2106, we examined the surface properties of the catalytic domains of the four phosphatases (Fig. 4). MKP-1 and MKP-3 displayed similar surface properties in the neighborhood of the active site. In particular, there was a concave region surrounded by hydrophobic residues on both structures, where the hydrophobic groups of the compounds tended to be positioned. Cdc25B and VHR, on the other hand, exhibited a

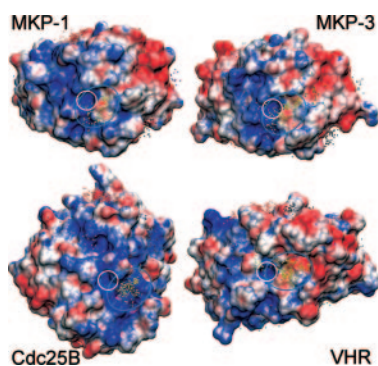


Fig. 4. Surface properties of dual specificity phosphatases and potential binding sites of small molecule inhibitors are displayed. The surface representations are colored on the basis of the solvent-exposed surface electrostatic potential calculated using APBS (Baker et al., 2001). Red and blue correspond to negatively and positively charged (or polar) regions, respectively, and white refers to neutral (or hydrophobic) regions. Each dot corresponds to the centroid of a binding pose for a compound, and there are 600 hundred poses for each phosphatase. Catalytic cavities are encircled in white. The clusters in the neighborhood of the catalytic sites are colored yellow and are encircled in blue. The poses in the second and third most distinctive clusters are shown in red and gray, respectively. Note the difference in the polarity/hydrophobicity of the surface within the blue circles, pointing to the origin of the differences in the selectivity of the small molecules against these DSPs. The diagrams were generated using VMD (Humphrey et al., 1996).

significantly more polar/charged character near the catalytic site. The Cdc25B active site was essentially basic, whereas VHR showed mostly acidic and some hydrophobic character. We then conducted unbiased molecular docking simulations in which the 10 active compounds were docked without any predefined binding site to the four protein phosphatases using AutoDock. Thirty docking runs were performed for both enantiomers of each compound, leading to a total of 600 poses for each phosphatase. The centroids of all poses are displayed in Fig. 4 to identify potential binding sites where the small molecules cluster. Notably, at least three potential binding sites were predicted for the 10 active compounds, with one of them being near the catalytic cysteine, and are seen enclosed in the blue ellipse.

Docking poses were found to cluster at hydrophobic regions and large cavities on the surface. Clusters were determined using an agglomerative clustering scheme and are colored differently. The poses closest to catalytic sites are shown in yellow. These are proposed to form the bound conformations that can potentially exhibit competitive inhibition. Based on the comparative analysis of these binding surfaces in the four DSPs, we speculated that the greater inhibitory action for MKP-1 and MKP-3 of the 10 compounds might be associated with the hydrophobic nature of the surface near their active site. The centers of the clusters closest to the catalytic site were further used as the center of biased search space using GOLD. The recurrent features observed in the docking poses of PSI2106 from these biased docking simulations were interactions of aromatic moieties of PSI2106 with the aromatic side chains of residues His²²⁹ and Phe²⁹⁹, in addition to a number of hydrophobic contacts involving residues Ala²⁶⁰ and Ile²⁶² and the β -carbons of Ser²⁶³ and Asn²⁹⁸ illustrated in Fig. 5 for MKP-1. Comparable interactions were observed with MKP-3. Cdc25B and VHR, on the other hand, lacked this type of hydrophobic interactions. Apparently, shape complementarity, rather than the specificity of interactions, played a major role in selecting the binding site near the catalytic cysteine.

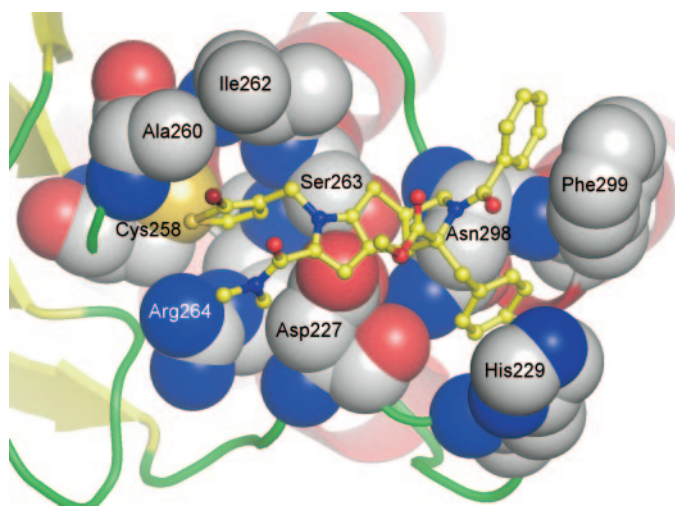


Fig. 5. Space-filling representation of MKP-1 active site bound to PSI2106 shown in ball and stick representation. The lowest energy pose was selected from 100 poses generated using GOLD with a flexible side-chain option. The key residues directly interacting with PSI2106 are labeled. His²²⁹ and Phe²⁹⁹ were predicted to have important roles in defining the bound conformation of PSI2106. The figure was generated using PyMol (DeLano Scientific LLC, Palo Alto, CA).

Discussion

Unlike the serine/threonine phosphatases, which have large numbers of potent small molecule inhibitors, mostly natural products, the tyrosine phosphatases and the DSPs in particular have few inhibitors. Pentamidine (Pathak et al., 2002) and sanguinarine (Vogt et al., 2005) have been reported to be in vitro inhibitors of MKP-1, but they are not selective and sanguinarine is not very potent. The benzofuran NU-126 showed some selectivity for MKP-1 compared with MKP-3, which supported the theoretical argument that differences in the amino acid composition would support selective inhibitors (Lazo et al., 2006). Nonetheless, NU-126 was not very potent with an IC_{50} value for MKP-1 of almost 30 μM (Lazo et al., 2006). The newly identified pyrrole carboxamides are structurally unique from previously known MKP-1 inhibitors. PSI2106 and MDF2085, which have IC_{50} values below 10 μM , showed >5-fold selectivity for human MKP-1 over MKP-3 and a much greater preference for MKP-1 over Cdc25B, PTP1B, or VHR. Their reversible inhibition was consistent with a covalent adduct- or redox-independent inhibitory mechanism, which separates these compounds from other reported inhibitors of DSPs.

The identification of 10 active compounds in the discovery library of 172 suggested that the pyrrole carboxamide pharmacophore could be an attractive chemical platform for future analog development. It is interesting to compare this active compound ratio with that seen with a more traditional focused library. We recently found 100 active compounds after screening 65,239 diverse small molecules from the National Institutes of Health repository (<http://pubchem.ncbi.nlm.nih.gov/assay/assay.cgi?aid=374>), which was a positive ratio that was 40-fold less than that seen with the pyrrole carboxamide library. Furthermore, the pyrrole carboxamide core structure was not identified in the National Institutes of Health diverse small molecule library, indicating the value of our focused library. The ability of two of the library compounds to inhibit the dephosphorylation of phosphorylated Erk also suggested that they could be useful. It should be noted, however, that the compounds appear to be much better inhibitors of the dephosphorylation of OMFP than of the protein substrate phosphorylated Erk. This may reflect the altered MKP conformation that is thought to occur after binding to their cognate substrate (Camps et al., 1998; Zhou et al., 2001), which is probably not recapitulated by OMFP. We have attempted to evaluate the ability of PSI2106 and MDF2085 to inhibit MKP-1 in cells using previously described cell-based assays (Vogt et al., 2005), including one that has been modified using a tetracycline-regulated promoter and will be described elsewhere. We did not, however, observe any evidence for MKP-1 inhibition. We considered the possibility that this lack of cellular activity might be due to high serum protein binding properties that were predicted by QikProp (Table 4), but we have observed significant growth inhibition of A549 cells cultured in the presence of 10% fetal bovine serum with PSI2106 ($IC_{50} = 5.3 \pm 2.8 \mu\text{M}$; $n = 2$) and MDF2085 ($IC_{50} = 4.4 \pm 1.2 \mu\text{M}$; $n = 2$). Thus, both compounds have biological activity in the presence of serum. We have not yet linked A549 cell growth inhibition to cellular MKP-1 inhibition, however, and we have not seen growth

inhibition with HeLa cells under similar conditions. Additional mechanistic studies of these pyrrole carboxamides are warranted.

Because of the highly conserved protein tyrosine phosphatase active site, it was originally thought that selective inhibitors would not be obtainable. A strategy has been proposed, however, in which a substrate might bind to the active site, the phospho-Tyr-binding site, and then to a peripheral site. Indeed, some protein tyrosine phosphatase inhibitors do possess two pharmacophore subunits tethered together via a conformationally mobile linker (Puius et al., 1997). It is enticing to think that some of these 10 compounds are active because they contain two pharmacologically interesting subunits: a pyrrole carboxamide and a substituted proline. Documentation of this theory, however, will require additional studies, which it is hoped will be aided by the molecular modeling already conducted.

In summary, we believe these results illustrate the potential of the pyrrole carboxamide library for future pharmacological studies. Selective and potent inhibitors of MKP-1 would be valuable reagents to deconstruct the cellular role of this phosphatase in inflammation and neoplasia and might provide the chemical foundation for the development of new anticancer agents.

Acknowledgments

We appreciate our constructive discussions with members of the University of Pittsburgh Center for Chemical Methodologies and Library Development, the Drug Discovery Institute, and the Pittsburgh Molecular Library Screening Center, in particular Drs. Peter Wipf, Elizabeth R. Sharlow, Paul A. Johnston, and Andreas Vogt.

References

- Arnold D, Foster C, Huryn D, Lazo J, Johnston P, and Wipf P (2007) Synthesis and biological activity of a focused library of mitogen-activated protein kinase phosphatase inhibitors. *Chem Biol Drug Design* **69**:23–30.
- Baker N, Sept D, Joseph S, Holst M, and McCammon J (2001) Electrostatics of nanosystems: application to microtubules and the ribosome. *Proc Natl Acad Sci U S A* **98**:10037–10041.
- Brisson M, Nguyen T, Wipf P, Joo B, Day BW, Skoko JS, Schreiber EM, Foster C, Bansal P, and Lazo JS (2005) Redox regulation of Cdc25B by cell-active quinolinediones. *Mol Pharmacol* **68**:1810–1820.
- Brummond K, Curran D, Mitasev B, and Fischer S (2005) Heterocyclic α -alkylidene cyclopentenones obtained via a Pauson-Khand reaction of amino-acid derived allenynes: a scope and limitation study directed towards the preparation of a tricyclic pyrrole library. *J Org Chem* **70**:1745–1753.
- Camps M, Nichols A, Gillieron C, Antonsson B, Muda M, Chabert C, Boschert U, and Arkininstall S (1998) Catalytic activation of the phosphatase MKP-3 by ERK2 mitogen-activated protein kinase. *Science* **280**:1262–1265.
- Denkert C, Schmitt WD, Berger S, Reles A, Pest S, Siebert A, Lichtenegger W, Diel M, and Hauptmann S (2002) Expression of mitogen-activated protein kinase phosphatase-1 (MKP-1) in primary human ovarian carcinoma. *Int J Cancer* **102**:507–513.
- Duffy EM and Jorgensen WL (2000) Prediction of properties from simulations: free energies of solvation in hexadecane, octanol, and water. *J Am Chem Soc* **122**:2878–2888.
- Humphrey W, Dalke A, and Schulten K (1996) VMD—visual molecular dynamics. *J Mol Graphics* **14**:33–38.
- Jeong D, Yoon T, Kim J, Shim M, Jeong S, Son J, Ryu S, and Kim S (2006) Crystal structure of the catalytic domain of human MAP kinase phosphatase 5: structural insight into constitutively active phosphatase. *J Mol Biol* **360**:945–955.
- Jones G, Willett P, Glen R, Leach A, and Taylor R (1997) Development and validation of a genetic algorithm for flexible docking. *J Mol Biol* **267**:727–748.
- Jorgensen WL (2004) The many roles of computation in drug discovery. *Science* **303**:1813–1818.
- Lazo JS, Aslan DC, Southwick EC, Cooley KA, Ducruet AP, Joo B, Vogt A, and Wipf P (2001) Discovery and biological evaluation of a new family of potent inhibitors of the dual specificity protein phosphatase Cdc25. *J Med Chem* **44**:4042–4049.
- Lazo JS, Nunes R, Skoko JJ, de Oliveira PEQ, Vogt A, and Wipf P (2006) Novel benzofuran inhibitors of human mitogen-activated protein kinase phosphatase-1. *Bioorg Med Chem* **14**:5643–5650.
- Liao Q, Guo J, Kleeff J, Zimmermann A, Buchler MW, Korc M, and Friess H (2003) Down-regulation of the dual-specificity phosphatase MKP-1 suppresses tumorigenicity of pancreatic cancer cells. *Gastroenterology* **124**:1830–1845.

- Magi-Galluzzi C, Mishra R, Fiorentino M, Montironi R, Yao H, Capodiceci P, Wishnow K, Kaplan I, Stork PJ, and Loda M (1997) Mitogen-activated protein kinase phosphatase 1 is overexpressed in prostate cancers and is inversely related to apoptosis. *Lab Invest* **76**:37–51.
- Morris G, Goodsell D, Halliday R, Huey R, Hart W, Belew R, and Olson AJ (1998) Automated docking using a Lamarckian genetic algorithm and an empirical binding free energy function *J Comput Chem* **19**:1639–1662.
- Nyati M, Feng F, Maheshwari D, Varambally S, Zielske S, Ahsan A, Chun P, Arora V, Davis M, Jung M, et al. (2006) Ataxia telangiectasia mutated down-regulates phospho-extracellular signal-regulated kinase 1/2 via activation of MKP-1 in response to radiation. *Cancer Res* **66**:11554–11559.
- Okano K, Tokuyama H, and Fukuyama T (2006) Total synthesis of (+)-yatakemycin. *J Am Chem Soc* **128**:7136–7137.
- Pathak MK, Dhawan D, Lindner DJ, Borden EC, Farver C, and Yi T (2002) Pentamidine is an inhibitor of PRL phosphatases with anticancer activity. *Mol Cancer Ther* **1**:1255–1264.
- Puius Y, Zhao Y, Sullivan M, Lawrence D, Almo S, and Zhang Z (1997) Identification of a second aryl phosphate-binding site in protein-tyrosine phosphatase 1B: a paradigm for inhibitor design. *Proc Natl Acad Sci U S A* **94**:13420–13425.
- Sali A and Blundell T (1993) Comparative protein modelling by satisfaction of spatial restraints. *J Mol Biol* **234**:779–815.
- Stockwell BR (2004) Exploring biology with small organic molecules. *Nature* **432**:846–854.
- Vogt A, Tamewitz A, Skoko J, Sikorski RP, Giuliano KA, and Lazo JS (2005) The benzo[c]phenanthridine alkaloid, sanguinarine, is a selective, cell-active inhibitor of mitogen-activated protein kinase phosphatase-1. *J Biol Chem* **280**:19078–19086.
- Wang HY, Cheng Z, and Malbon CC (2003) Overexpression of mitogen-activated protein kinase phosphatases MKP1, MKP2 in human breast cancer. *Cancer Lett* **191**:229–237.
- Werner S, Iyer PS, Fodor MD, Coleman CM, Twining LA, Mitasev B, and Brummond KM (2006) Solution-phase synthesis of a tricyclic pyrrole-2-carboxamide discovery library applying a Stetter-Paal-Knorr reaction sequence. *J Comb Chem* **8**:368–380.
- Wu JJ and Bennett AM (2005) Essential role for mitogen-activated protein (MAP) kinase phosphatase-1 in stress-responsive MAP kinase and cell survival signaling. *J Biol Chem* **280**:16461–16466.
- Zhou B, Wu L, Shen K, Zhang J, Lawrence DS, and Zhang ZY (2001) Multiple regions of MAP kinase phosphatase 3 are involved in its recognition and activation by ERK2. *J Biol Chem* **276**:6506–6515.

Address correspondence to: Dr. John S. Lazo, Pittsburgh Molecular Libraries Screening Center, Department of Pharmacology, University of Pittsburgh Drug Discovery Institute, Biomedical Science Tower-3, Suite 10040, 3401 Fifth Ave., University of Pittsburgh, Pittsburgh, PA 15260. E-mail: lazo@pitt.edu
